Environmental Research Letters

LETTER

Pan American interactions of Amazon precipitation, streamflow, and tree growth extremes

D W Stahle[1] , M C A Torbenson[2], I M Howard[1], D Granato-Souza[1] , A C Barbosa[3], S Feng[1], J Schöngart[4], L Lopez[5], R Villalba[5], J Villanueva[6] and K Fernandes[1,7]

1   University of Arkansas, Fayetteville, AR, United States of America
2   Ohio State University, Columbus, United States of America
3   Federal University of Lavras, Lavras, Brazil
4   INPA National Institute for Amazon Research, Manaus, Brazil
5   Instituto Argentino de Nivología, Glaciología y Ciencias Ambientales, CONICET, Mendoza, Argentina
6   INIFAP, Gomez Palacio, Durango, Mexico
7   International Research Institute for Climate and Society, Columbia University, Palisades, NY, United States of America

E-mail: dstahle@uark.edu

Keywords: Amazon, Pan American climate, tree-ring chronologies, Cedrela odorata, ENSO

Abstract

Rainfall and river levels in the Amazon are associated with significant precipitation anomalies of opposite sign in temperate North and South America, which is the dominant mode of precipitation variability in the Americas that often arises during extremes of the El Niño/Southern Oscillation (ENSO). This co-variability of precipitation extremes across the Americas is imprinted on tree growth and is detected when new tree-ring chronologies from the eastern equatorial Amazon are compared with hundreds of moisture-sensitive tree-ring chronologies in mid-latitude North and South America from 1759 to 2016. Pan-American co-variability exists even though the seasonality of precipitation and tree growth only partially overlaps between the Amazon and mid-latitudes because ENSO forcing of climate can persist for multiple seasons and can orchestrate a coherent response, even where the growing seasons are not fully synchronized. The tree-ring data indicate that the El Niño influence on inter-hemispheric precipitation and tree growth extremes has been strong and stable over the past 258-years, but the La Niña influence has been subject to large multi-decadal changes. These changes have implications for the dynamics and forecasting of hydroclimatic variability over the Americas and are supported by analyses of the available instrumental data and selected climate model simulations.

1. Introduction

The El Niño/Southern Oscillation (ENSO) has a strong influence on the spatial structure of precipitation variability across the tropical to temperate latitudes of North and South America [1–5]. El Niño conditions tend to induce drought over the eastern Amazon Basin and Nordeste region of Brazil, simultaneously with wetness over the mid-latitudes of both North and South America. This out-of-phase tropical to temperate pattern is the leading mode of precipitation variability in the Americas in gridded instrumental observations and in precipitation simulations based on the Community Earth System Models-Last Millennium Ensemble (CESM-LME; [6]). Hemispheric scale Pan American precipitation patterns exhibit decadal variability in the

CESM-LME simulations and may be more robust during warm rather than cold sea surface temperature (SST) conditions in the tropical Pacific. High-resolution climate proxies from the Amazon, in combination with tree-ring data from the extra-tropical Americas, could help document the high and low frequency interactions of Pan American precipitation during prehistory.

Exactly dated, climate sensitive tree-ring chronologies record regional moisture anomalies and large-scale ENSO teleconnections in the extra-tropical Americas [7–10], but annual growth rings suitable for tree-ring chronology development are rare in tropical forests and long precipitation-sensitive chronologies have not existed in the Amazon Basin until recently [11–13]. Two ring-width chronologies of *Cedrela odorata* have been developed in the eastern

equatorial Amazon spanning the past 231- to 258-years, both exhibiting the same calendar year dating and tree growth response to wet season rainfall totals in the eastern Amazon [13, 14].

In this article we demonstrate that tree-ring reconstructed wet season precipitation extremes in the eastern equatorial Amazon are coherent with tree growth and reconstructed precipitation anomalies of opposite sign in the mid-latitudes of North and South America. This co-variability of Pan American precipitation and tree growth is driven primarily by ENSO, especially El Niño conditions, and exists even though the seasonality of precipitation and tree growth only partially overlaps between the Amazon and middle latitudes. The new tree-ring chronologies from the equatorial Amazon provide the proxy data needed to investigate extremes and low-frequency variability in these hemispheric connections and indicate differences in the strength of the El Niño and La Niña influence on coherent Pan American precipitation patterns during the instrumental and pre-instrumental periods.

2. Data and methods

The tree-ring chronologies used in these analyses were developed from *C. odorata* at two locations in the Rio Paru basin of the northeastern Amazon, Rio Paru Alto (RPA, 0°58'36"S, 53°19'33"W; [13]) and Rio Paru Baixo (RPB, 0°59'51"S, 53°16"W; [14]). The Rio Paru and several other large streams drain an area of the Guiana Shield in the northeastern Amazon covering over $400\,000$ km^2 extending from the Amazon River north across the drainage divide into the Guyanas. This area is roughly the size of California and preserves one of the largest, most isolated, and pristine tropical rainforests left on earth [15], with the tallest trees yet discovered in the Amazon Basin (>80 m in height; [16]). *C. odorata* is native to these old-growth forests and this valuable rainforest species can form annual growth rings suitable for the long-term reconstruction of regional rainfall totals.

Cross sections salvaged from legally harvested logs were dried, highly polished, and the annual growth rings were dated to the exact calendar year of formation with the Douglas method of cross-dating [17]. The annual rings were precisely measured (0.01 mm) and sequential inter-series correlation analyses in the computer program COFECHA [18] were used to evaluate dating and measurement accuracy. Data adaptive cubic smoothing splines were used for detrending each ring-width series in order to minimize growth excursions that are not consistent between trees and likely reflect non-climatic stand dynamics in these closed canopy rain forests (flexible splines with a 50% frequency response of 100-years were used for detrending; [14, 19]). The robust mean index RPA chronology is based on 27 radii from 10

trees and dates from 1786 to 2016 [13, 19]. The RPB chronology uses 50 radii from 22 trees, dating from 1759 to 2016 [14].

The RPB chronology was used to reconstruct wet season (Feb-Jul) precipitation totals for a 1x1° regional average near Santarem, Brazil (0–1°S, 56–57°W; [14]). The regional precipitation observations were obtained from the Global Precipitation Climatology Centre-Full Dataset [20]. Because the reconstruction just involved the rescaling of the RPB chronology to regional precipitation using bivariate regression [14], the extreme years are identical whether based on the original ring-width chronology or the derived reconstruction. These RPB ring width and reconstructed precipitation extremes in the eastern Amazon are both used to compare with tree growth and precipitation anomalies across the Americas during the instrumental and pre-instrumental periods.

The existing RPA chronology of *C. odorata* [13] is only used for comparison with the RPB data in these analyses. The RPA chronology is well correlated with the RPB time series, has a similar wet season precipitation signal [14], and the RPA extremes are coherent with tree growth and precipitation in the extra-tropical Americas. But the RPA chronology is not as long (1786–2016) and the climate response is not as strong as the signal observed in the RPB time series.

The RPB chronology from the eastern Amazon and the derived wet season precipitation reconstruction [14] were compared with the publically available tree-ring chronologies from North and South America using both composite and correlation analyses. The mid-latitude chronologies were obtained from the International Tree-Ring Data Bank (ITRDB; [21]), National Centers for Environmental Information (NCEI), NOAA Paleoclimatology Program (www.ncdc.noaa.gov/data-access/paleoclimatology-data). All chronologies were de-trended and standardized [19], in some cases by the original contributors and in others specifically for this study. De-trending is designed to minimize non-climatic effects associated with the increasing size and age of the sample trees. Standardization removes differences in absolute growth rates for the unbiased calculation of the mean index chronology. Temporal changes in sample size and tree age can induce variance trend in the mean index chronology so the variance of these chronologies was also de-trended using the methods of Meko *et al* [22].

Pan American precipitation patterns were investigated with gridded standardized precipitation indices (SPI) for North and South America from the Global Precipitation Climatology Center Full Dataset (GPCC_FD; [20]) extending from 1891 to 2016 at a resolution of $2.5 \times 2.5°$ (i.e. 1 month SPI averaged seasonally, 2.5° resolution used to facilitate

cartographic comparison with the tree-ring data). The Amazon tree-ring chronologies and wet season precipitation reconstruction were compared with the GPCC data and with the gridded (0.5°) tree-ring reconstructions of cool season (Dec-Apr) SPI included in the North American Seasonal Precipitation Atlas (NASPA; [23]). ENSO influence on Pan American precipitation and tree growth was investigated using the Climate Prediction Center's Oceanic Niño Index for the Niño 3.4 region.

Singular spectrum analysis (SSA; [24, 25]) was used to quantify the multi-decadal variability that dominates the reconstruction (the leading 35.4-year SSA waveform represents 20% of the time series variance; band width = 20). The extreme high and low growth years in this RPB chronology from 1772–1978 (upper and lower 10th percentiles) were used to compute composite means for the hundreds of tree-ring chronologies from North and South America available from the ITRDB (note that sample size is low in the RPB chronology before 1772 and many chronologies in the ITRDB end in 1978). There were 21 years in the upper, and 21 years in the lower 10th percentile in the RPB chronology from 1772–1978. Monte Carlo resampling (n = 10 000) of each chronology was used to estimate the one-tailed significance thresholds for the individual tree-ring chronology composite means over North and South America during extremes of tree growth in the eastern Amazon. The reconstructed wet season (Feb-Jul) precipitation extremes computed by Granato-Souza *et al* [14] were also compared with the gridded cool season SPI reconstructions in the NASPA during their common interval from 1759–2016 (also 1772–2016) using composite and correlation analyses (note that the gridded Dec-Apr SPI values in the NASPA are based entirely on instrumental observations after 1978; [23]). Two tailed Students t-tests were used to estimate the significance of grid point mean SPI during extremes of reconstructed rainfall in the eastern Amazon.

In addition to the inter-hemispheric comparisons of the tree-ring data, we include analyses of the monthly precipitation observations made at Manaus (3°08'30"N, 60°01'W) from 1901 to 2016 [note that the homogeneity of the wet season totals at Manaus during the early 20th century are suspect [14] and the missing monthly values for 1909 were replaced with the monthly medians]. The annual maximum river level observations of the Rio Negro at Manaus from 1903 to 2016 are also used for composite and correlation analyses of the GPCC and NASPA precipitation data sets. The monthly precipitation simulations computed with the CESM-LME were used to provide a model perspective on multi-decadal variability of Pan American precipitation and ENSO forcing.

3. Results

The tree-ring reconstruction of wet season precipitation in the eastern Amazon is plotted from 1772–2016 in figure 1(a). The reconstruction is well replicated during this 1772–2016 interval, exhibits strong multi-decadal variability, and the driest years are associated with El Niño conditions in the tropical Pacific [14]. Several two- to three-year droughts in the lowest 10th percentile occurred consecutively during prolonged El Niño events that are well documented in the instrumental record. These persistent El Niño events include the famous 1876–1878 and 1982–1983 episodes that were associated with pan-tropical drought, crop failure, and famine [26–28], simultaneously with record wet conditions in the mid-latitude Americas (e.g. [29]). Multi-decadal variability of Amazonian hydroclimate has been identified in instrumental observations and climate model simulations [30–34], in the composite Amazon-Rio Negro river level data (e.g. [35]), and in high and low resolution paleoclimate data [12, 36]. This quasi-periodic low frequency variability may also impact the inter-hemispheric co-variability of precipitation extremes in the Americas.

Rainfall over the eastern Amazon is associated with precipitation anomalies of opposite sign in mid-latitude North and South America in the GPCC instrumental SPI for the period from 1950 to 2016. The leading mode of variance in principal components analyses [37] of instrumental October-March precipitation totals in the Americas is this pattern of tropical to extra-tropical anti-phasing (PC1; figure 1(b); also noted in [2]). October-March was used because ENSO influences on Pan American precipitation are important during this season, but similar PCA results were computed for February-July precipitation, which is the wet season for the eastern Amazon (not shown). Dry (wet) conditions in the eastern Amazon tend to co-occur with wetness (dryness) over extra-tropical North and South America, and this pattern represents 12% of the variance in instrumental October-March precipitation (see also [2]). The annual maximum river level of the Rio Negro at Manaus (1903–2016), which integrates wet season precipitation over a vast basin (691 000 km^2) in the northern Amazon, is also negatively correlated with precipitation over mid-latitude North and South America (figure 1(c)). This correlation between Rio Negro maxima and October-March precipitation is most notable over Mexico and the southwestern United States, and is a strong hydroclimatic manifestation of the ENSO influence on Pan American precipitation.

These large-scale inter-hemispheric precipitation and streamflow connections are recorded by the available tree-ring chronologies for the Americas. When
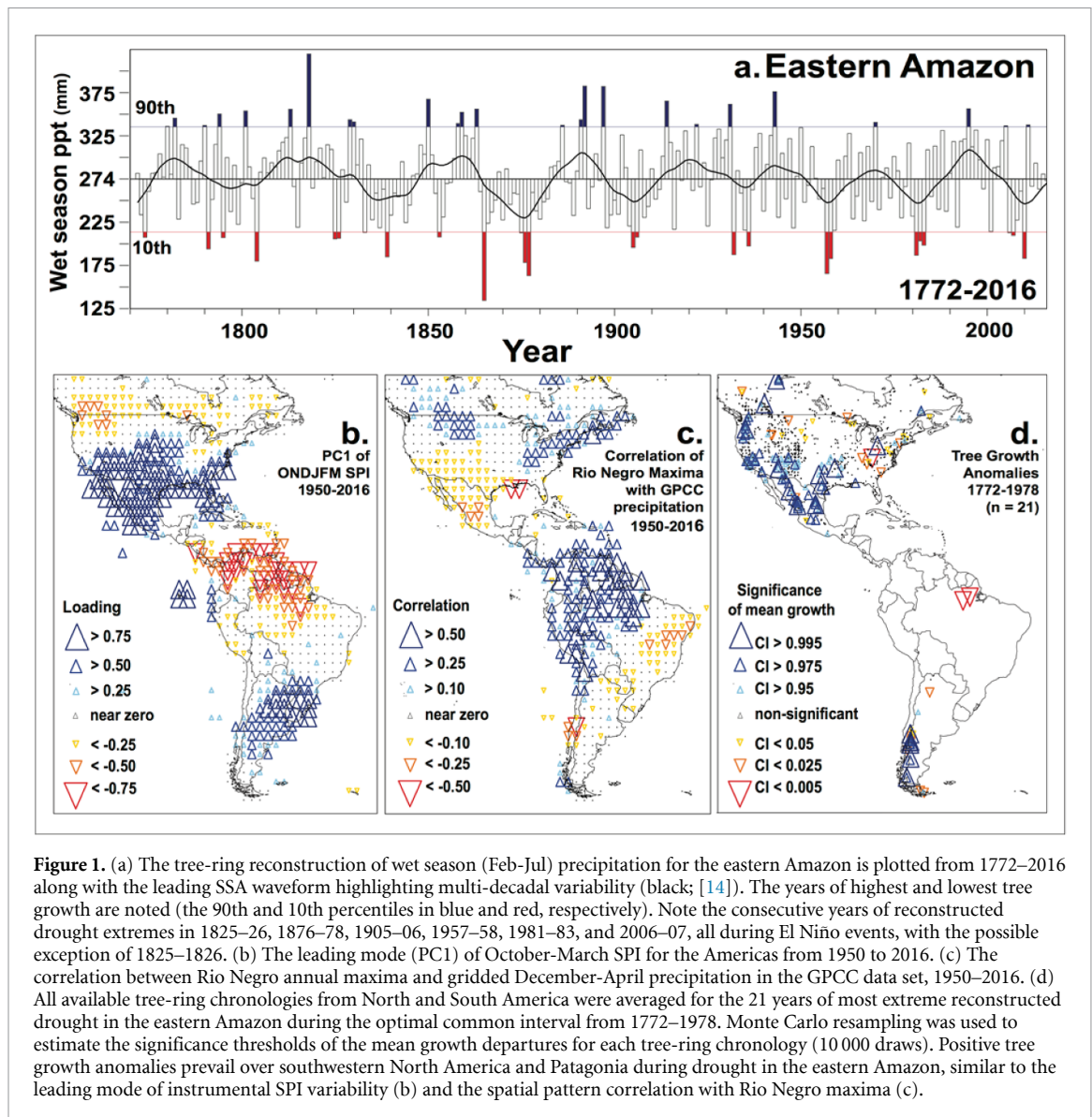
Figure 1. (a) The tree-ring reconstruction of wet season (Feb-Jul) precipitation for the eastern Amazon is plotted from 1772–2016 along with the leading SSA waveform highlighting multi-decadal variability (black; [14]). The years of highest and lowest tree growth are noted (the 90th and 10th percentiles in blue and red, respectively). Note the consecutive years of reconstructed drought extremes in 1825–26, 1876–78, 1905–06, 1957–58, 1981–83, and 2006–07, all during El Niño events, with the possible exception of 1825–1826. (b) The leading mode (PC1) of October-March SPI for the Americas from 1950 to 2016. (c) The correlation between Rio Negro annual maxima and gridded December-April precipitation in the GPCC data set, 1950–2016. (d) All available tree-ring chronologies from North and South America were averaged for the 21 years of most extreme reconstructed drought in the eastern Amazon during the optimal common interval from 1772–1978. Monte Carlo resampling was used to estimate the significance thresholds of the mean growth departures for each tree-ring chronology (10 000 draws). Positive tree growth anomalies prevail over southwestern North America and Patagonia during drought in the eastern Amazon, similar to the leading mode of instrumental SPI variability (b) and the spatial pattern correlation with Rio Negro maxima (c).

the 21 years of lowest tree growth in the RPB tree-ring chronology (i.e. 10th percentile; figure 1(a)) are used to composite the hundreds of chronologies available in the ITRDB for the well replicated common period of 1772–1978, highly significant above average growth is observed in many chronologies across southwestern North America and temperate South America (i.e. northern Patagonia, figure 1(d)). The 21 years of highest tree growth in the Amazon are not consistently matched with low growth anomalies over North America, but significant below average growth is observed over Patagonia when just the 11 most extreme high growth years in the Amazon are used to compute these composite maps (i.e. 5th percentile; not shown). The new *Cedrela* chronologies from the eastern Amazon, in conjunction with the mid-latitude chronologies, may therefore represent useful proxies of the co-variability of Pan American precipitation extremes, especially when drought and low tree growth occurred in the eastern Amazon.

The identification of Pan American symmetry in tree growth and reconstructed precipitation extremes relies on the exact calendar year dating of the tree-ring data from both the tropics and mid-latitudes. The accuracy and precision of the tree-ring dated chronologies in mid-latitude North and South America were demonstrated decades ago, but the formation of clear annual rings in tropical tree species is much less common and development of exactly dated chronologies has been more difficult. The co-occurrence of low tree growth extremes in the eastern Amazon with significant positive growth anomalies in temperate tree-ring chronologies from the Americas provides strong evidence that the dating of *Cedrela* ring-width series from the triple canopy rainforests of the Amazon is indeed exact. In fact, the *Cedrela* low growth extremes are anti-phased with some of the most rigorously dated and repeatedly validated tree-ring chronologies yet developed. In North America these include blue oak (*Quercus douglasii*) at Mt. Diablo, California; ponderosa pine (*Pinus ponderosa*) from Santa Fe, New

Mexico; and Douglas-fir (*Pseudotsuga menziesii*) at El Salto in the state of Durango, Mexico. In South America, 23 of 25 *Nothofagus pumilio* chronologies exhibit significant coherence during low growth over the Amazon, including the chronology from Cerro Diego de León near San Carlos de Bariloche, Argentina. The exact dating of the master tree-ring chronology of *C. odorata* from the Rio Paru has significant practical value for dendrochronology and will leverage the development of additional tree-ring chronologies from the Amazon.

The inter-hemispheric co-variability of instrumental precipitation appears to be largely forced by ENSO (e.g. [1–3]). When gridded instrumental SPI are averaged for the February-May portion of the wet season in the eastern Amazon during the seven most extreme El Niño events from 1950 to 2016, below average precipitation prevailed over the eastern Amazon and northeast Brazil simultaneously with above average precipitation in the mid-latitudes of both North and South America (figure 2(a)). February-May precipitation was used because these totals represent much of the wet season most important to tree growth in the eastern Amazon, as well as a portion of the season of strongest ENSO influence over the Americas, but similar results are observed for the October-March and October-May seasons. When the instrumental precipitation data are averaged for the seven most extreme La Niña events, an opposite though somewhat weaker pattern of precipitation anomalies prevailed, especially over western North America (figure 2(b)).
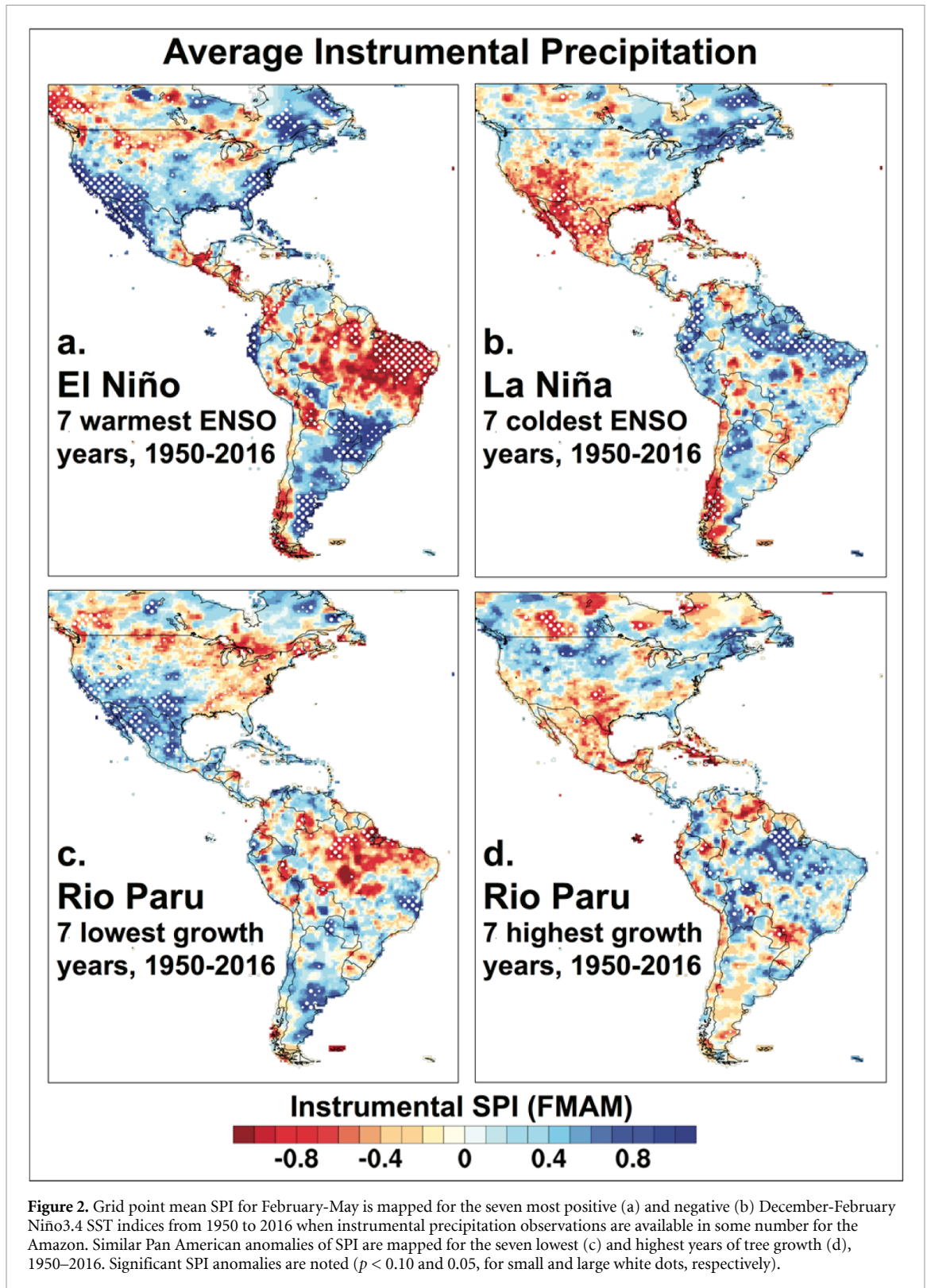
Inter-hemispheric symmetry is also reproduced when the seven lowest and seven highest years of *Cedrela* growth in the eastern Amazon from 1950 to 2016 are used to composite the GPCC instrumental precipitation data for the Americas (figures 2(c) (d)). In this case the Rio Paru Baixo *Cedrela* chronology represents a proxy for drought and wetness in the eastern Amazon (i.e. low vs high growth extremes, respectively) and the larger Pan American response of precipitation to ENSO. However, the wet mid-latitude SPI anomalies are stronger during Amazon drought/low growth often associated with El Niño conditions than the North American drought pattern observed during Amazon wetness/high growth typical of La Niña events (figures 2(c) (d)). The coherent Pan American anomalies of annual precipitation, streamflow, and surface air temperature (Oct-Sep; [2]) are also stronger during warm ENSO conditions. However, the tree growth response to drought conditions tends to be more consistent than the response to extreme wetness [7], which may dilute the Pan American tree growth response to La Niña forcing of wetness over the eastern Amazon, as well as the El Niño forcing of wetness over the mid-latitudes of North and South America.

The CESM-LME simulations of October-March precipitation over North and South America are dominated by anti-phasing between the eastern equatorial Amazon and the mid-latitudes, and the simulated PC1 time series exhibits pronounced decadal variability (figures 3(a) (b)). The Pan American interaction of precipitation is also stronger during warm ENSO events when composite maps of the CESM-LME precipitation simulations are compared during warm and cold SST extremes in the Niño 3.4 region of the tropical Pacific (figures 3(c) (d)). This observed and simulated inter-hemispheric response to ENSO appears to be largely responsible for the spatial pattern of observed and simulated loadings on PC1 for October-March precipitation across the Americas (figures 1(b) and 3(b)).

The coherent Pan American response to precipitation and tree growth extremes in the eastern Amazon is well documented in tree-ring data from North America, in part because the North American proxies are numerous, cover most of the continent, and have been used to develop skillful temporal and spatial reconstructions of drought indices and seasonal precipitation totals [23, 38]. Composite maps of gridded cool season precipitation reconstructions (Dec-Apr SPI) available in the NASPA indicate a significant wet response over southwestern North America (SW NAM) during the 25 driest extremes in the eastern Amazon from 1772 to 2016, typical of El Niño conditions (figure 4(a)), and consistent with the response of the individual tree-ring chronologies depicted in figure 1(d). The anomalies of cool season SPI during the 25 wettest years in the eastern Amazon are below average but are not significant over most of North America (figure 4(b)), indicating that the coherent Pan American response to cold ENSO conditions was not strong from 1772 to 2016, likely due in part to the weak La Niña response in the available tree-ring data from the eastern Amazon. However, the tree-ring data suggest that the response to cold ENSO conditions in the eastern Amazon and the anti-phasing of reconstructed precipitation over North America may have been stronger during the pre-instrumental period before 1880.

When the list of reconstructed drought extremes for the Amazon is divided before and after 1880 (i.e. the pre-instrumental and instrumental periods), there is a significant above average precipitation response over SW NAM during both periods typical of El Niño conditions (1772–1880 and 1881–2016; figures 4(c), (e)). However, the North American SPI averages for the wettest years in the eastern Amazon are quite different during these two subperiods. Significant and widespread dryness occurred over SW NAM during the 13 eastern Amazon wet extremes from 1772 to 1880, typical of La Niña forcing (figure 4(d)). But near normal SPI is computed over SW NAM during the 12 Amazon wet years after 1880, and reconstructed SPI was in fact above average over California and Nevada (figure 4(f)). Near normal conditions over SW NAM are also observed

Figure 2. Grid point mean SPI for February-May is mapped for the seven most positive (a) and negative (b) December-February Niño3.4 SST indices from 1950 to 2016 when instrumental precipitation observations are available in some number for the Amazon. Similar Pan American anomalies of SPI are mapped for the seven lowest (c) and highest years of tree growth (d), 1950–2016. Significant SPI anomalies are noted ($p < 0.10$ and 0.05, for small and large white dots, respectively).

when the wettest years in the Manaus rain gage (1901–2016) are used to composite the instrumental GPCC December-April precipitation data, even though significant wetness is observed over SW NAM during the drought years at Manaus (composite maps not shown).

Correlation analyses between hydroclimatic variables in the Amazon and precipitation over North America during subperiods of the instrumental and pre-instrumental eras indicate multi-decadal variability in the interactions of Pan American precipitation extremes. Reconstructed rainfall totals in the eastern Amazon were correlated with the gridded December-April precipitation reconstructions for North America for six non-overlapping ≈ 44-year subperiods from 1759 to 2016 (figures 5(a)–(f); using

Figure 3. (a) The first principal component (PC1) time series of October-March precipitation totals in the CESM- Last Millennium Ensemble simulations over the Americas is plotted for the simulated years from 850–1850 (gray) along with a smoothed version (black; smoothing spline with a 50% frequency response of 10 years). (b) The loadings on PC1 of the CESM-LME simulations are mapped. The mean October-March SPI anomalies are also mapped during the (c) warmest and (d) coolest years in the Nino 3.4 region of the tropical Pacific (upper and lowest 10th percentiles for Oct-May SSTs), based on the CESM-LME simulations. Similar results are computed using an October-July season for both SSTs and SPI.
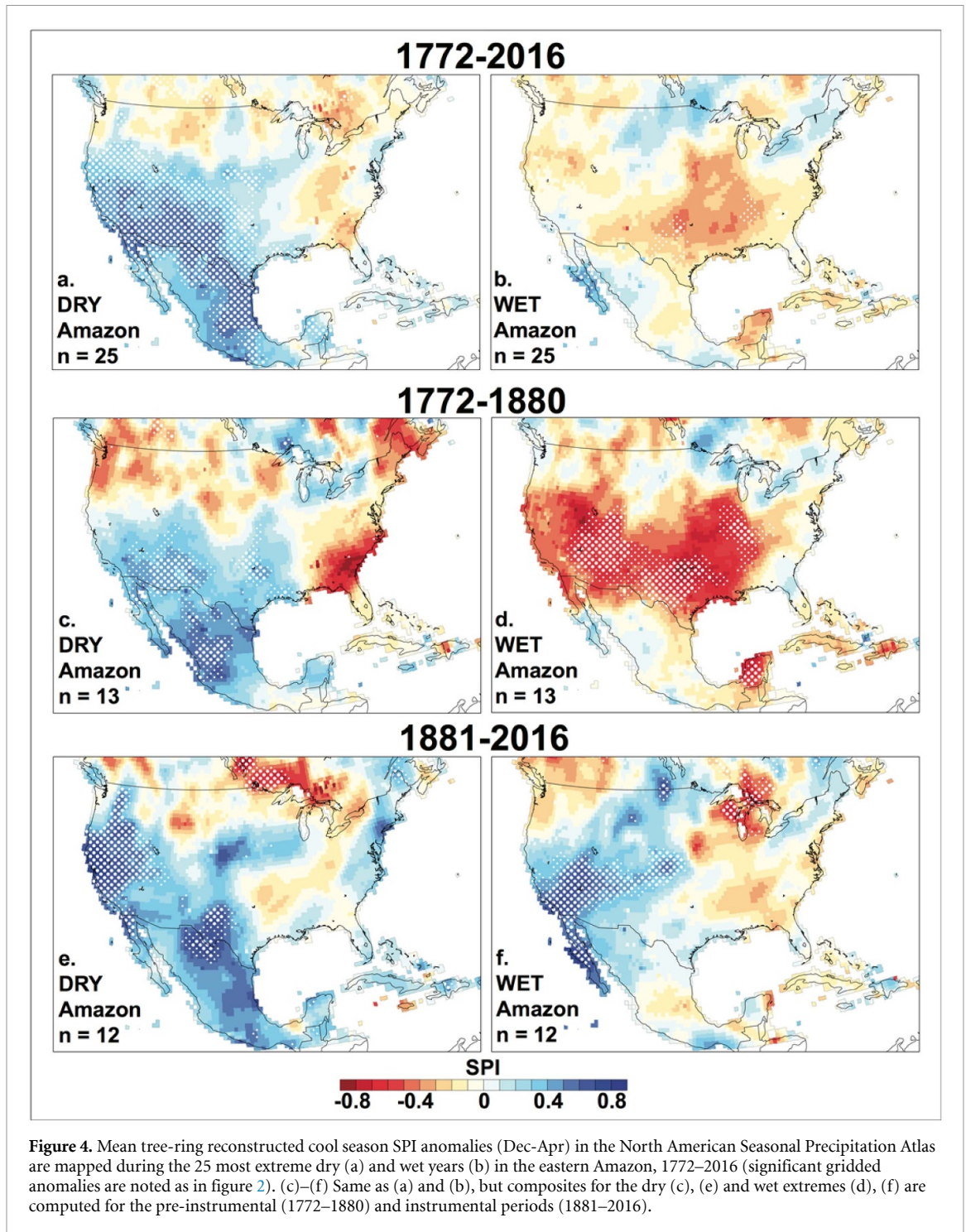
the entire reconstruction for the eastern Amazon, along with reconstructed SPI from 1759 to 1891 and instrumental SPI from 1892 to 2016 available in the NASPA; [23]). Strong negative correlations are observed over portions of SW NAM for four of the six subperiods (figures 5(a)–(c), (f)). Negative correlations are observed over central Mexico from 1892–1931 to 1932–1974, but only a few of the grid point correlations are significant (figures 5(d), (e)). Significant correlations with reconstructed Amazon rainfall are then again computed widely over Mexico and Texas for the most recent subperiod (1975–2016; figure 5(f)).

The multi-decadal changes in correlation between rainfall over the Amazon and precipitation anomalies over SW NAM are not confined to the tree-ring data. When the instrumental wet season (Feb-Jul) precipitation data for Manaus are correlated with the
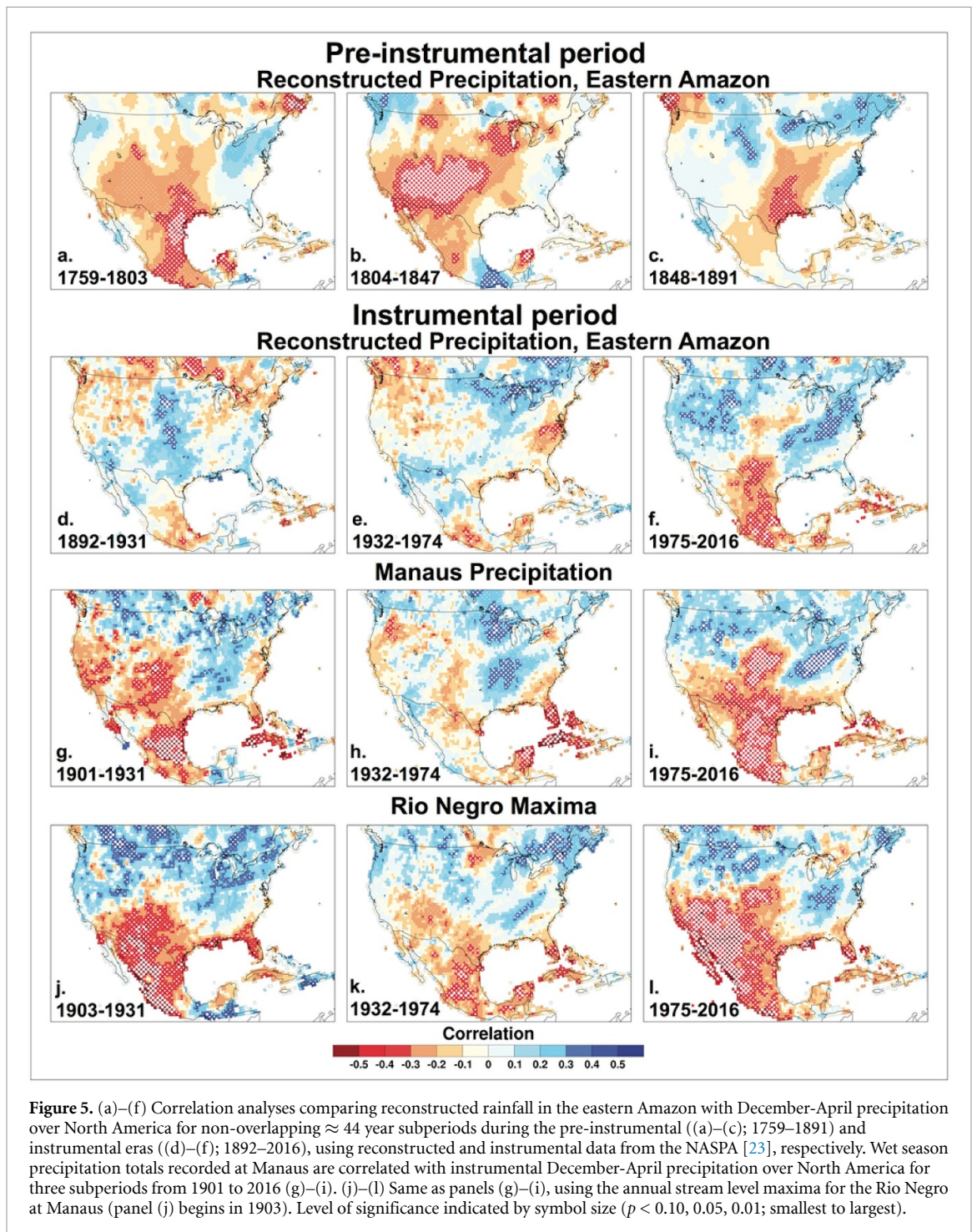
instrumental December-April SPI for North America for three subperiods of the instrumental era, there is a significant and widespread wet response in cool season precipitation over SW NAM during the early (1901–1931) and late subperiods (1975–2016), but not during the mid-20th century (1932–1974; figures 5(g)–(i)). The annual river level maxima recorded for the Rio Negro at Manaus from 1903 to 2016 are also negatively correlated with December-April precipitation totals over SW NAM (figures 5(j)–(l)), but these correlations with the Rio Negro also weakened during the mid-20th century (figure 5(k)).

The instrumental and proxy data all indicate that the precipitation co-variability between the Amazon and SW NAM weakened during the mid-20th century (1932–1974; figures 5(e), (h), (k)). However, reconstructed rainfall in the eastern Amazon is not

Figure 4. Mean tree-ring reconstructed cool season SPI anomalies (Dec-Apr) in the North American Seasonal Precipitation Atlas are mapped during the 25 most extreme dry (a) and wet years (b) in the eastern Amazon, 1772–2016 (significant gridded anomalies are noted as in figure 2). (c)–(f) Same as (a) and (b), but composites for the dry (c), (e) and wet extremes (d), (f) are computed for the pre-instrumental (1772–1880) and instrumental periods (1881–2016).

highly correlated with instrumental precipitation over SW NAM during the early 20th century (1892–1931; figure 5(d)) even though Manaus precipitation and Rio Negro maxima are significantly correlated with precipitation over SW NAM from 1901 (1903) to 1931 (figures 5(g), (j)). The reason for this difference between the proxy and instrumental data during the early 20th century is not clear, and the correlation with reconstructed precipitation in the Amazon does not improve when restricted to the 1901–1931 period (not shown). Nevertheless, the reconstruction for the eastern Amazon is significantly correlated with

precipitation over portions of SW NAM during the pre-instrumental period (1759–1891; figures 5(a)–(c)) and during the recent period from 1975 to 2016 when the Manaus rainfall and Rio Negro maxima are most strongly correlated with SW NAM precipitation (figures 5(f), (i), (l)). Consequently, the long instrumental precipitation and streamflow series from the central Amazon, and the proxy tree-ring data from the eastern Amazon, along with the CESM-LME precipitation simulations for the Americas, indicate that the Pan American co-variability of precipitation has been subject to multi-decadal variability. Dettinger

Figure 5. (a)–(f) Correlation analyses comparing reconstructed rainfall in the eastern Amazon with December-April precipitation over North America for non-overlapping $\approx$ 44 year subperiods during the pre-instrumental ((a)–(c); 1759–1891) and instrumental eras ((d)–(f); 1892–2016), using reconstructed and instrumental data from the NASPA [23], respectively. Wet season precipitation totals recorded at Manaus are correlated with instrumental December-April precipitation over North America for three subperiods from 1901 to 2016 (g)–(i). (j)–(l) Same as panels (g)–(i), using the annual stream level maxima for the Rio Negro at Manaus (panel (j) begins in 1903). Level of significance indicated by symbol size ($p < 0.10, 0.05, 0.01$; smallest to largest).

et al [2, 3] demonstrated that some of the low-frequency variability in Pan American hydroclimatology was related to ENSO.

4. Discussion and conclusions

The co-variability of precipitation across North and South America is imprinted on tree growth in equatorial and extra-tropical forests. Tree-ring reconstructed drought extremes in the eastern Amazon are linked with observed and reconstructed wet conditions across Mexico and the Southwest from

1759 to 2016 (figure 4(a)). This Pan American climate coherence is driven largely by ENSO and is documented for the first time based on tree-ring chronologies from the eastern Amazon. Only two long *Cedrela* chronologies are available for the eastern Amazon, but they are sufficient to indicate significant Pan American co-variability of reconstructed precipitation during the 18th and 19th centuries, prior to the advent of instrumental meteorological observations.

The anti-phasing of precipitation and tree growth anomalies from tropical to temperate latitudes in the Americas is detected in the tree ring data in

spite of differences in the season of precipitation response. Many North American tree-ring chronologies are correlated with cool season precipitation prior to growth (Dec–Apr) due to winter precipitation recharge of soil moisture. Consequently, there is some overlap with the seasonal growth response of *Cedrela* in the eastern Amazon to wet season rainfall from February to July. The growing season in northern Patagonia is typically from November to March so it is only partly simultaneous with the wet season in the eastern Amazon. But because ENSO forcing of precipitation over the Americas can persist for multiple seasons it can orchestrate a coherent tree growth response in widely different regions, even where the growing seasons are not fully synchronized.

The Rio Negro river level record is arguably the most important hydroclimatic time series in the Amazon, given the length, internal homogeneity, and the catchment-wide integration of precipitation that it represents. Rio Negro maximum stream levels are negatively correlated with December-April precipitation over a large sector of Mexico and the southwestern United States. This significant extratropical correlation is higher than observed using the single station precipitation totals at Manaus or the single site reconstruction of precipitation in the eastern Amazon, likely due to precipitation integration over the huge Rio Negro basin in the northern Amazon. This suggests that the paleoclimate record of Pan American precipitation co-variability will be improved if a wider geographical array of moisture sensitive tree-ring chronologies can be developed for the Amazon. The strong mid-latitude precipitation correlation with Rio Negro maxima also suggests that these Pan American climate interactions may not be restricted to just El Niño and La Niña extremes, but might involve additional dynamics associated with the meridional overturning of the atmosphere in the Hadley Circulation.

derived reconstruction of wet season precipitation for the eastern Amazon, and the instrumental and reconstructed cool season precipitation data in the NASPA are available at the NOAA Paleoclimatology Program.

Data availability statement

The data that support the findings of this study are openly available at the following URL/DOI: www.ncdc.noaa.gov/data-access/paleoclimatology-data. Data will be available from 15 October 2020.

ORCID iDs

D W Stahle ⓘ https://orcid.org/0000-0002-8943-2541
D Granato-Souza ⓘ https://orcid.org/0000-0002-7011-0892
K Fernandes ⓘ https://orcid.org/0000-0001-8160-0769

References

[1] Dai A, Fung I Y and Del Genio A D 1997 Surface observed global land precipitation variations during 1900–88 *J. Clim.* **10** 2943–62

[2] Dettinger M D, Cayan D R, McCabe G C and Marengo J A 2000 Multiscale streamflow variability associated with El Niño/Southern Oscillation *El Niño and the Southern Oscillation-Multiscale Variability and Global and Regional Impacts*, ed H F Diaz and V Markgraf (Cambridge: Cambridge University Press) pp 113–46

[3] Dettinger M D, Battisti D S, McCabe G C, Bitz C M and Garreaud R D 2001 Interhemispheric effects of interannual and decadal ENSO-like climate variations on the Americas *Present and past Interhemispheric Climate Linkages in the Americas and Their Societal Effects*, ed V Markgraf (New York: Academic) pp 58–80

[4] Villalba R, D'Arrigo R D, Cook E R, Wiles G and Jacoby G C 2001 Decadal-scale climatic variability along the extratropical western coast of the Americas: evidences from tree-ring records *Present and past Interhemispheric Climate Linkages in the Americas and Their Societal Effects*, ed V Markgraf (New York: Academic) pp 155–72

[5] Yeh S W *et al* 2018 ENSO atmospheric teleconnections and their response to greenhouse gas forcing *Rev. Geophys.* **56** 185–206

[6] Otto-Bliesner B L, Brady E C, Fasullo J, Jahn A, Landrum L, Stevenson S, Rosenbloom N, Mai A and Strand G 2016 Climate variability and change since 850 C.E.: an ensemble approach with the Community Earth System Model (CESM) *Bull. Am. Meteor. Soc.* 735–54

[7] Fritts H C 1976 *Tree Rings and Climate* (London: Academic)

[8] Cook E R, Seager R, Cane M A and Stahle D W 2007 North American drought: reconstructions, causes, and consequences *Earth Sci. Rev.* **81** 93–134

[9] Christie D A, Lara A, Barichivich J, Villalba R, Morales M S and Cug E 2009 El Niño-Southern oscillation signal in the world's highest-elevation tree-ring chronologies from the Altiplano, Central Andes *Palaeogeog. Palaeoclim. Palaeoeco.* **281** 309–19

[10] Torbenson M C A, Stahle D W, Howard I M, Burnette D J, Villanueva J, Cook E R and Griffin D 2019 Multidecadal modulation of the ENSO teleconnection to precipitation and tree growth over subtropical North America *Paleoceanogr. Paleoclimatol.* **34** 886–900

[11] Brienen R J W, Helle G, Pons T L, Guyot J-L and Gloor M 2012 Oxygen isotopes in tree rings are a good proxy for Amazonian precipitation and ENSO variability *Proc. Nat Acad. Sci.* **109** 16957–62

[12] Lopez L, Stahle D W, Villalba R, Torbenson M C A, Feng S and Cook E R 2017 Tree-ring reconstructed rainfall over the Southern Amazon Basin *Geophys. Res. Lett.* **44** 7410–8

[13] Granato-Souza D, Stahle D W, Barbosa A C, Feng S, Torbenson M C A, Pereira G, Schongart J, Barbosa J P and Griffin D 2019 Tree rings and rainfall in the equatorial Amazon *Clim. Dyn.* **52** 1857–69

[14] Granato-Souza D, Stahle D W, Torbenson M C A, Howard I M, Barbosa A C, Feng S and Schongart J 2020 Multi-decadal changes in wet season precipitation totals over the eastern Amazon *Geophys. Res. Lett.* **47** e2020GL087478

[15] Rull V, Vegas-Vilarrubia T and Safont E 2016 The Lost World's pristinity at risk *Divers. Distrib.* **22** 995–9

[16] Gorgens E B, Motta A Z, Assis M, Nunes M H, Jackson T, Coomes D, Rosette J, Aragão L E O E C and Ometto J P 2019 The giant trees of the Amazon basin *Frontiers Ecol. Environ.* **17** 373–4

[17] Douglass A E 1941 Crossdating in dendrochronology *J. Forestry* **39** 825–31

[18] Holmes R L 1983 Computer-assisted quality control in tree-ring dating and measurement *Tree-Ring Bull.* **43** 69–78

[19] Cook E R and Kariukstis L (eds.) 1990 *Methods of Dendrochronology: Applications in the Environmental Sciences* (Berlin: Springer)

[20] Becker A, Finger P, Meyer-Christoffer A, Rudolf B, Schamm K, Schneider U and Ziese M 2013 A description of the global land-surface precipitation data products of the Global Precipitation Climatology Centre with sample applications including centennial (trend) analysis from 1901–present *Earth Syst. Sci. Data* **5** 71–99

[21] Zhao S, Pederson N, D'Orangeville L, Hillerislambers J, Boose E, Penone C, Bauer B, Jiang Y and Manzanedo R D 2019 The International Tree-Ring Data Bank (ITRDB) revisited: data availability and global ecological representativity *J. Biogeogr.* **46** 355–68

[22] Meko D M, Cook E R, Stahle D W, Stockton C W and Hughes M K 1993 Spatial patterns of tree growth anomalies in the United States and southeastern Canada *J. Clim.* **6** 1773–86

[23] Stahle D W *et al* 2020 Dynamics, variability, and change in seasonal precipitation reconstructions for North America *J. Clim.* **33** 3173–95

[24] Ghil M *et al* 2002 Advanced spectral methods for climatic time series *Rev. Geophys.* **40** 1–41

[25] St. George S and Ault T R 2011 Is energetic decadal variability a stable feature of the central Pacific Coast's winter climate? *J. Geophys. Res.* **116**

[26] Glantz M H 2001 *Currents of Change: Impacts of El Niño and La Niña on Climate and Society* (Cambridge: Cambridge University Press)

[27] Aceituno P, Del Rosario Prieto M, Solari M E, Martínez A, Poveda G and Falvey M 2007 The 1877–1878 El Niño episode: associated impacts in South America *Clim. Change* **92** 389–416

[28] Singh D, Seager R, Cook B I, Cane M, Ting M, Cook E R and Davis M 2018 Climate and the global famine of 1876-78 *J. Clim.* **31** 9445–67

[29] Quiroz R S 1983 The climate of the "El Nino" winter of 1982-83, a season of extraordinary climatic anomalies *Mon. Wea. Rev.* **111** 1685–706

[30] Labat D, Ronchail J, Callede J, Guyot J L, De Oliveira E and Guimaraes W 2004 Wavelet analysis of Amazon hydrological regime variability *Geophys. Res. Lett.* **31** L02501

[31] Marengo J A 2009 Long-term trends and cycles in the hydrometeorology of the Amazon basin since the late 1920s *Hydrol. Process.* **23** 3236–44

[32] Wang G, Sun S and Mei R 2011 Vegetation dynamics contributes to the multi-decadal variability of precipitation in the Amazon region *Geophys. Res. Lett.* **38** L19703

[33] Ault T, Cole J E and St. George S 2012 The amplitude of decadal to multidecadal variability in precipitation simulated by state-of-the-art climate models *Geophys. Res. Lett.* **39** L21705

[34] Fernandes K, Giannini A, Verchot L, Baethgen W and Pinedo-Vasquez M 2015 Decadal covariability of Atlantic SSTs and western Amazon dry-season hydroclimate in observations and CMIP5 simulations *Geophys. Res. Lett.* **42** 6793–801

[35] Barichivich J, Gloor M, Peylin P, Brienen R J W, Schongart J, Espinoza J C and Pattnayak K C 2018 Recent intensification of Amazon flooding extremes driven by strengthened Walker circulation *Sci. Adv.* **2018** eaat8785

[36] Wang X, Edwards R L, Auler A S, Cheng H, Kong X, Wang Y, Cruz F W, Dorale J A and Chiang H W 2017 Hydroclimate changes across the Amazon lowlands over the past 45,000 years *Nature* **541** 204–7

[37] Jolliffe I T 2002 *Principal Component Analysis* (Berlin: Springer)

[38] Cook E R, Seager R, Heim R R, Vose R S, Herweijer C and Woodhouse C A 2010 Megadroughts in North America: placing IPCC projections of hydroclimatic change in a long-term paleoclimate context *J. Quat. Sci.* **25** 48–61

Pan American interactions of Amazon precipitation, streamflow, and tree growth extremes

To cite this article: D W Stahle *et al* 2020 *Environ. Res. Lett.* **15** 104092

View the article online for updates and enhancements.